Desalination and Water Treatment
www.deswater.com
doi: 10.5004/dwt.2022.28530

262 (2022) 235–247
June

Investigation of the methylene blue adsorption onto waste perlite

Uğur Selengil, Derya Yıldız*

Eskişehir Osmangazi University, Chemical Engineering Department, Eskişehir, Turkey, Tel. +90 222 239 37 50; email: uselen@ogu.edu.tr, ORCID: 0000-0003-2576-1343 (U. Selengil), email: dozcan@ogu.edu.tr, ORCID: 0000-0002-5628-8424 (D. Yıldız)

Received 18 November 2021; Accepted 21 April 2022

ABSTRACT

In this study, the adsorption of methylene blue, a cationic dyestuff, on waste perlite was investigated. Waste perlite is the part of the perlite that remains unexpanded during the expansion process. The effects of pH, amount of adsorbent, contact time, initial concentration and temperature on the adsorption process were investigated. No significant difference was observed in dyestuff removal with the change of solution pH according to the obtained results. For this reason, all experimental studies were performed at the original pH of the solution (pH = 6.80). When the effect of the adsorbent dose was examined, it was determined that the most suitable adsorbent amount was 0.5 g for 50 mL of dyestuff solution at 100 mg/L concentration. In the adsorption experiments with a contact time of 24 h, it was observed that the system reached equilibrium in 7 h. It was observed that the adsorption kinetics of methylene blue on waste perlite fit the pseudo-second-order kinetic model. Maximum adsorption capacity of waste perlite was 9.91 mg/g at 0.5 g adsorbent and 100 mg/L dyestuff concentration for 50 mL solution volume. The adsorption data fit the Langmuir isotherm model. The thermodynamic data ($\Delta H°$, $\Delta S°$, $\Delta G°$) showed that this process is spontaneous and endothermic. At the end of this study, it was seen that the waste perlite is a suitable adsorbent for the removal of methylene blue from wastewater.

Keywords: Adsorption; Adsorption parameters; Dyestuff adsorption; Expanded perlite; Unexpanded perlite; Methylene blue

1. Introduction

The wastewater problem has gradually increased with the acceleration of industrialization in the 20th century. Many industries, such as textiles, food and dyes, use dyestuffs and pigments for colouring the products. Colour is a visible contaminant in the wastewater of such industries. The presence of even a very small quantity of colouring matter (less than 1 ppm) is undesirable in water due to its appearance and environmental impacts. Biodegradation of dyestuffs in the environment is not easy due to their chemical structures and resistance to light and oxidation [1,2]. Methylene blue, an organic dyestuff, is used in many applications such as cotton and wool dyeing, paper dyeing and temporary hair dyeing [3,4]. The adsorption of methylene blue on solids is strong, so it is often used as a model compound in the removing studies of dyestuffs and organic contaminants from the aqueous solutions [5]. The most common technics for colour removal from wastewater are oxidation, coagulation/flocculation, precipitation, ion exchange and adsorption processes. However, these methods are only economical and effective in situations where solute concentrations are high [2,6,7]. Recent studies have shown that adsorption is an effective method for dyestuff removal [4,5,8–15]. This method is also an economical one if the adsorbent used for adsorption is cheap and readily available. For the dyestuff removal from wastewater, many materials such as ash [16], treatment sludges [13], zeolite [17], sepiolite [18,19], bentonite [11,20], rice

* Corresponding author.

husk [6], graphene [4], lignite [10] and activated carbon [9,21] have been used as adsorbents in the previous studies. In recent years, expanded and unexpanded perlite has also been used in the adsorption studies [2,22–26]. The perlite, formed by the cooling of volcanic eruption, is an amorphous rock with rich silica content. It contains 72%–75% silica, 12%–15% Al_2O_3, 4%–5% K_2O, 2%–4% Na_2O and generally 2%–6% water. When raw perlite is heated to 750°C–1,100°C, it can be expanded to thirty times. Thus, expanded perlite with a light and porous structure is obtained [25,27,28]. Expanded perlite has many advantages such as low density, low toxicity, non-corrosivity, high surface area, good mechanical resistance, low thermal conductivity, high chemical and thermal stability, low cost and ease of use [28–30]. Expanded perlite is widely used in building materials, concrete [27,31,32], fire bricks, ceramics, glass, paints, food, medicine and fuel oil [33–35]. Perlite has also attracted attention with its sorption properties due to its high silica content. The sorption behaviour of perlite depends on the Si–OH, which are silanol groups formed by silicon atoms on the perlite surface [30]. The waste material remaining unexpanded during the expanded perlite production is called "waste perlite".

In this study, the waste perlite was obtained from a factory that is producing expanded perlite, and it is used as an adsorbent for methylene blue adsorption from aqueous solutions. In this way, waste management will be ensured by using unexpanded perlite, which is considered as waste. It will also be evaluated for an alternative adsorbent for the removal of pollutants in wastewater. For this purpose, the effects of adsorbent dosage, pH contact time, temperature and initial concentration were investigated, and the data obtained were evaluated in order to reveal the kinetics and thermodynamics of the adsorption process.

2. Materials and methods

2.1. Characterization of waste perlite

The waste perlite used in this study was obtained from a factory producing expanded perlite in Kütahya (Türkiye). The size of the waste perlite particles used in the adsorption experiments were under 0.080 mm (80 μm) and the waste perlite samples had approximately 1% moisture content. The specific surface area, micropore volume, mesopore volume and average pore diameter of the waste perlite were determined by using the Brunauer–Emmett–Teller (BET) method. For this purpose, a Quantachrome Autosorb 1C device was used to measure the nitrogen gas adsorption (77 K). The adsorption of inert gases method is generally used to determine the pore structures of porous materials. In this method, the waste perlite sample was kept at 200°C under vacuum for 12 h and made ready for analysis. The N_2 adsorption isotherm was obtained in the range of 10^{-2} to 1 relative pressure (P/P_0). The surface area (S_{BET}) of the sample was calculated by the BET equation in the relative pressure range of 0.01–0.15. The external surface area and micropore volume were calculated by using the *t*-plot method. The total pore volume was calculated from the amount of N_2 adsorbed at a relative pressure of approximately equal to 1. The mesopore volume was calculated by subtracting the micropore volume from the total pore volume. Barrett–Joyner–Halenda method was applied to determine the pore size distribution and adsorption isotherm of perlite. The chemical composition of waste perlite was determined by the Panalytical ZETIUM XRF device, the surface morphology and surface texture of waste perlite was examined using Hitachi Regulus 8230 FE-SEM scanning electron microscopy.

2.2. Adsorption experiments

The effects of pH, contact time, adsorbent amount, initial concentration and temperature on the adsorption of methylene blue on perlite waste were investigated.

Methylene blue is a cationic (basic) dyestuff with a molecular formula of $C_{16}H_{18}ClN_3S$. Its molecular weight is 319.85 g/mol. It is not considered to be acutely toxic, but has various destructive effects on health and the environment [12].

The methylene blue used in the experiments was obtained from Merck. A 1 g portion of methylene blue was dissolved in distilled water and the solution was diluted to 1 L in a volumetric flask. Thus, a 1,000 mg/L methylene blue stock solution was prepared. Solutions of various concentrations used in the experimental studies were prepared from this stock solution by dilution. The solutions were prepared in a concentration range of 5–100 mg/L. The absorbance values of these solutions were determined using a UV spectrophotometer (Shimadzu UV-120-01) at a wavelength of 663 nm, and the working line was prepared.

Five samples were prepared from the methylene blue solution with the initial concentration of C_0 = 100 mg/L and a volume of 50 mL to investigate the effect of pH on adsorption. The pH values of the solutions were adjusted with NaOH and HCl solutions in the pH range of 2–10. The pH values of the solutions measured with the ISTEK Neomet 220L pH meter. On each of the solutions, 0.5 g of waste perlite was added. The adsorption experiments were carried out in a shaking water bath (Memmert WNB22) at 25°C for 24 h. In other group of experiments, the same procedure was applied with the addition of 0.1, 0.3, 0.5, 0.7 and 1.0 g of waste perlite to each flask in order to determine the effect of adsorbent dose. To examine the effect of contact time, 0.5 g of waste perlite were added to each of the methylene blue solutions with an initial concentration of 100 mg/L and a volume of 50 mL, and the flasks containing the solutions were kept in a shaking water bath at 25°C for different periods (30 min–24 h). Ten different methylene blue solutions in a volume of 50 mL with concentrations varying between 10–100 mg/L were prepared from the stock solution to investigate the effect of initial concentration, and the same procedure was applied with the addition of 0.5 g waste perlite to each solution under the same conditions. To investigate the effect of temperature, 0.5 g waste perlite was added to each solution, of which the methylene blue concentration was 100 mg/L and the volume was 50 mL; and the solutions were shaken at 25°C, 35°C and 45°C in a water bath for 24 h.

At the end of each experiment, the solutions were taken into the tubes and centrifuged, and the absorbances of the clear solution samples were read in the UV

spectrophotometer. The remaining methylene blue concentration (C_e) in the solution was calculated. The amounts of methylene blue adsorbed per gram of waste perlite (q_e) and the removal percentages were calculated from Eq. (1) and from Eq. (2), respectively.

$$q_e = \frac{V \times \left(C_0 - C_e\right)}{m} \tag{1}$$

$$\text{Removal}\left(\%\right) = \frac{C_0 - C_e}{C_0} \times 100 \tag{2}$$

In these equations the amount of dyestuff adsorbed on unit adsorbent is q_e (mg/g), initial concentration of dye in solution is C_0 (mg/L), concentration of dyestuff remaining in solution after adsorption is C_e (mg/L), volume of solution is V (L) and mass of adsorbent is m (g).

2.3. Adsorption kinetics

Kinetic analysis allows to determine the mechanism of the adsorption process. Therefore, the pseudo-first-order, pseudo-second-order and intraparticle diffusion kinetic models were applied for the experimental data. The rate constant of the pseudo-first-order adsorption is determined from the following equation given by Lagergren [36,37]:

$$\ln\left(q_e - q\right) = \ln q_e - k_1 t \tag{3}$$

where q_e and q are the amount of dyestuff adsorbed (mg/g) at equilibrium and at any time t, respectively, and k_1 is the rate constant (h^{-1}) for the pseudo-first-order adsorption. The k_1 and q_e values were calculated from the slope and the intercept of the $\ln(q_e - q)$ vs. t plots, respectively (Fig. 9).

The pseudo-second-order equation based on the adsorption capacity is expressed as [37],

$$\frac{t}{q} = \frac{1}{k_2 q_e^{\,2}} + \frac{t}{q_e} \tag{4}$$

where q_e and q are the amounts of dyestuff adsorbed (mg/g) at equilibrium and any time t, respectively, and k_2 is the rate constant of the pseudo-second-order adsorption (g/mg h). The values of the pseudo-second-order model constants (q_e and k_2) were determined from the slope and intercept of the t/q vs. t-plot, respectively (Fig. 10). The intraparticle diffusion equation that changes with time's square root is expressed as follows [2,38],

$$q_t = k_i t^{1/2} + C \tag{5}$$

where q_t is the amount adsorbed at a given time (mg/g) t is time (min) and k_i (mg/g $\text{min}^{0.5}$) is the rate constant of intraparticle diffusion (Fig. 11). The k_1, k_2 and k_i values are found from the curves, the q_e values are calculated from the models and the correlation coefficients are given in Table 3.

2.4. Adsorption isotherms

Adsorption isotherms can explain the equilibrium relationship between adsorbents and adsorbates. Adsorption isotherms are essential for the analysis and design of adsorption systems. The Langmuir and Freundlich models are chosen because of their simplicity and compatibility with experimental data under various operating conditions. Generally, the Langmuir equation is designed for a homogeneous surface; good fit of these equations represents monolayer adsorption. On the other hand, its compatibility with the Freundlich isotherm model that is developed for a heterogeneous surface indicates the multilayer adsorption. [21]. In this study, experimental data were applied to the Langmuir and Freundlich isotherm equations. The Langmuir isotherm equation is represented by the following equation [36,39].

$$\frac{C_e}{q_e} = \frac{1}{Q_0 b} + \frac{C_e}{Q_0} \tag{6}$$

where C_e is the concentration of dyestuff at equilibrium (mg/L), q_e is the adsorbed amount at equilibrium (mg/g), b is the adsorption equilibrium constant (L/mg), and Q_0 is the adsorption capacity (mg/g). Langmuir adsorption isotherms at 25°C, 35°C and 45°C are given Fig. 13, and the values of b and Q_0 were calculated from the slope and intercept of the plot of C_e/q_e vs. C_e.

The R_L value, defined as below, is a dimensionless balance parameter [37,40].

$$R_L = \frac{1}{1 + bC_0} \tag{7}$$

Table 1
Physical properties of waste perlite

BET surface area (m^2/g)	12.93
Micropore area (m^2/g)	3.912
Total pore volume (cm^3/g)	0.01999
Micropore volume (cm^3/g)	0.00139
Mesopore volume (cm^3/g)	0.0186
Average pore diameter (nm)	6.183

Table 2
Chemical composition of waste perlite (%)

SiO_2	70.90
Al_2O_3	13.53
Fe_2O_3	1.49
TiO_2	0.13
CaO	1.19
MgO	0.28
Na_2O	2.53
K_2O	5.63
SO_3	0.08
LOI	4.24

LOI: loss on ignition

Table 3
Kinetic constants for pseudo-first-order, pseudo-second-order, and intraparticle diffusion

	Pseudo-first-order			Pseudo-second-order			Intraparticle diffusion		
q_e (mg/g) (experimental)	k_1 (h^{-1})	q_e (mg/g)	R^2	k_2 (g/mg h)	q_e (mg/g)	R^2	C	k_i (mg/g $min^{1/2}$)	R^2
							0.7943	0.5755	0.9962
9.9121	0.671	2.712	0.94	0.139	10.320	0.99	3.8053	0.2945	0.9985
							9.8577	0.0015	0.7193

where b is the Langmuir constant (L/g), and C_0 is the initial dyestuff concentration (mg/L). This parameter indicates whether the isotherm is unfavourable ($R_L > 1$), favourable ($R_L < 1$), linear ($R_L = 1$) or irreversible ($R_L = 0$) [4].

The Freundlich isotherm is defined by following equation [36].

$$\ln q_e = \ln K_f + \frac{1}{n}\ln C_e \tag{8}$$

where C_e indicates the concentration of dyestuff at equilibrium (mg/L), q_e is the adsorption capacity at equilibrium (mg/g), K_f (mg/g) is the Freundlich capacity constant, and n is the Freundlich density constant. The Freundlich isotherm plots at 25°C, 35°C and 45°C are given in Fig. 14, and the values of n and K_f were calculated from the intercept and the slope of the plot of $\ln q_e$ vs. $\ln C_e$.

2.5. Adsorption thermodynamics

The standard free energy change ($\Delta G°$), enthalpy change ($\Delta H°$) and entropy change ($\Delta S°$) of adsorption are calculated from the following equations:

$$K_d = \frac{m \times q_e}{C_e \times V} \tag{9}$$

$$\Delta G° = -RT \ln K_C \tag{10}$$

where R is the gas constant (8.314 J/mol K), K_d is the distribution coefficient [41], and T is the temperature in K. The standard enthalpy ($\Delta H°$) and entropy ($\Delta S°$) of adsorption can be estimated from the Van't Hoff equation [36].

$$\ln K_d = -\frac{\Delta H°}{RT} + \frac{\Delta S°}{R} \tag{11}$$

The $\Delta H°$ and $\Delta S°$ factors can be estimated from the slope and intercept of the $\ln K_d$ vs. $1/T$ plot, respectively and results are given at Table 6.

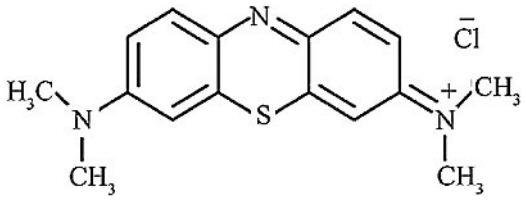

Fig. 1. Methylene blue.

3. Results and discussions

3.1. Characterization of waste perlite

The surface properties, the chemical composition and the surface morphology of the waste perlite were determined by using the BET, the X-ray fluorescence (XRF), Fourier-transform infrared spectroscopy (FTIR) and the scanning electron microscopy–energy-dispersive X-ray spectroscopy (SEM-EDS) methods respectively.

The physical properties of the waste perlite are seen in Table 1. According to the table, the mesopore volume constitutes a large part of the total pore volume (93%).

The adsorption–desorption isotherm and pore-size distribution of the waste perlite are given in Fig. 2. As seen in Fig. 2, the shape of the isotherm represent the Type IV according to the Brunauer, Deming and Teller (BDT) classification. Type IV isotherms indicate the presence of mesopore structure. The desorption branch in Fig. 2 also shows the hysteresis loop representing the development of mesoporosity. The pore size distribution of waste perlite dense is in the range of 10–65 Å. It showed a large peak at about 15 Å. Two more peaks were observed in the range of 15–35 Å and 36–62 Å. According to IUPAC, the porous structures are classified into three groups as microporous (<20 Å), mesoporous (20–500 Å) and macroporous (>500 Å). As seen from Table 1, the average pore diameter of waste perlite was found as 61.83 Å. According to these results, the waste perlite structure includes both micropores and mesopores, and mesopore volume is higher than micropore volume.

The chemical content of waste perlite was determined by the XRF method and the results are given in Table 2. According to the XRF analysis, the waste perlite contains high amounts of silica and alumina as well as alkali groups such as Na_2O and K_2O. It was seen that the main components of the waste perlite are 70.9% SiO_2 and 13.53% Al_2O_3.

While the perlite structure consists of compounds such as SiO_2, Al_2O_3, K_2O and Na_2O as the main components, TiO_2, CaO, MgO, Fe_2O_3, water and unburned carbon can also be found. Chemical analysis results were found to be similar in other studies with perlite [42–44].

The FTIR spectra of the waste perlite is given in Fig. 3.

The band seen at 3,637 cm^{-1} in the spectrum of waste perlite is attributed to the surface –OH groups of –Si–OH and water molecules adsorbed on the surface [42,45]. The peaks at 1,006 and 785 cm^{-1} are defined as the stretching vibration of Si–O–Si and Si–O–Al bonds [46,47]. The peak seen at 1,625 cm^{-1} in the perlite spectrum is characteristic of the water molecule [42,43,45]. Since waste perlite loses water with temperature in the expansion process, the intensity of

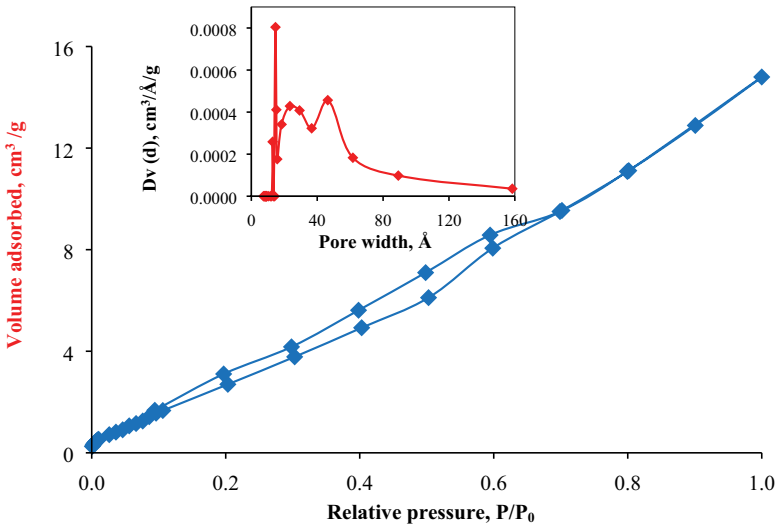

Fig. 2. Adsorption–desorption isotherm and pore-size distribution of waste perlite.

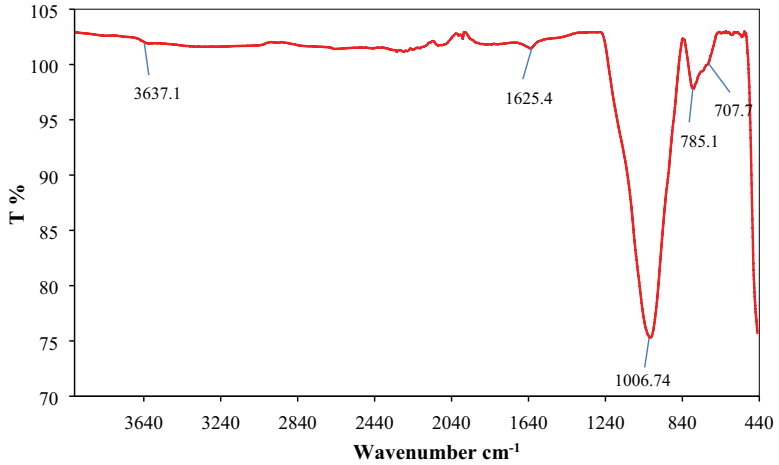

Fig. 3. FTIR spectra of the waste perlite.

this peak is lower than raw perlite [45]. The peak observed at 450 cm^{-1} is attributed to the bending vibration of the Si–O–Si bond [47,48].

The surface morphology and surface texture of waste perlite was examined using SEM. In order to determine the elemental content of the waste perlite, the EDS spectra and elementel mapping of the regions where the analysis was made on the surface were taken and results are given in Figs. 4 and 5.

According to the EDS results, waste perlite contains 43.26% O, 32.87% Si, 9.46% Al, 6.22% K, 4.44% Fe, and small amounts of Ca, Mg and Na by weight. The highest peaks seen in EDS are O, Si and Al. These results show that waste perlite is mainly composed of SiO_2 and Al_2O_3 as in XRF and FTIR. These results are also compatible with the literature [22,42,44,49–51]. In addition, with the elemental mapping given in Fig. 5, it was determined that Si, Al and O were homogeneously distributed on the surface of the waste perlite.

In Fig. 5a it is seen that the waste perlite surface has a sharp glassy structure with few pores. It is known that some of the perlite remains unexpanded during the expansion process. Although expanded perlite is very porous and in the form of thin plates, the unexpanded part has a smoother surface and amorphous structure [43,51,52]. Elemental mapping of perlite is also given in Fig. 5b. In elemental mapping, it has been seen that the main components in the composition of perlite are Si, O and Al.

3.2. Effect of pH

The adsorption efficiency depends on the solution pH. The dyestuff solution's initial pH affects the adsorbents' surface charge and the adsorbate's ionization degree. Therefore, pH is an important factor controlling dyestuff molecules' adsorption on adsorbent particles in solution [12]. Adsorption experiments were carried out at pH 2–11 at an initial concentration of 100 mg/L to observe the effect

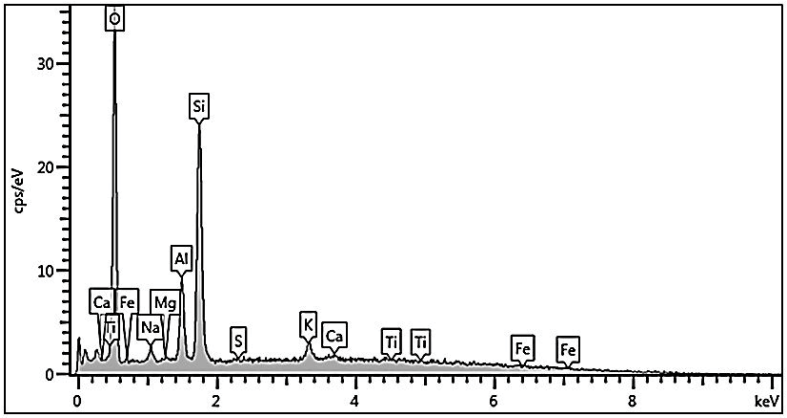

Fig. 4. EDS spectrum of waste perlite.

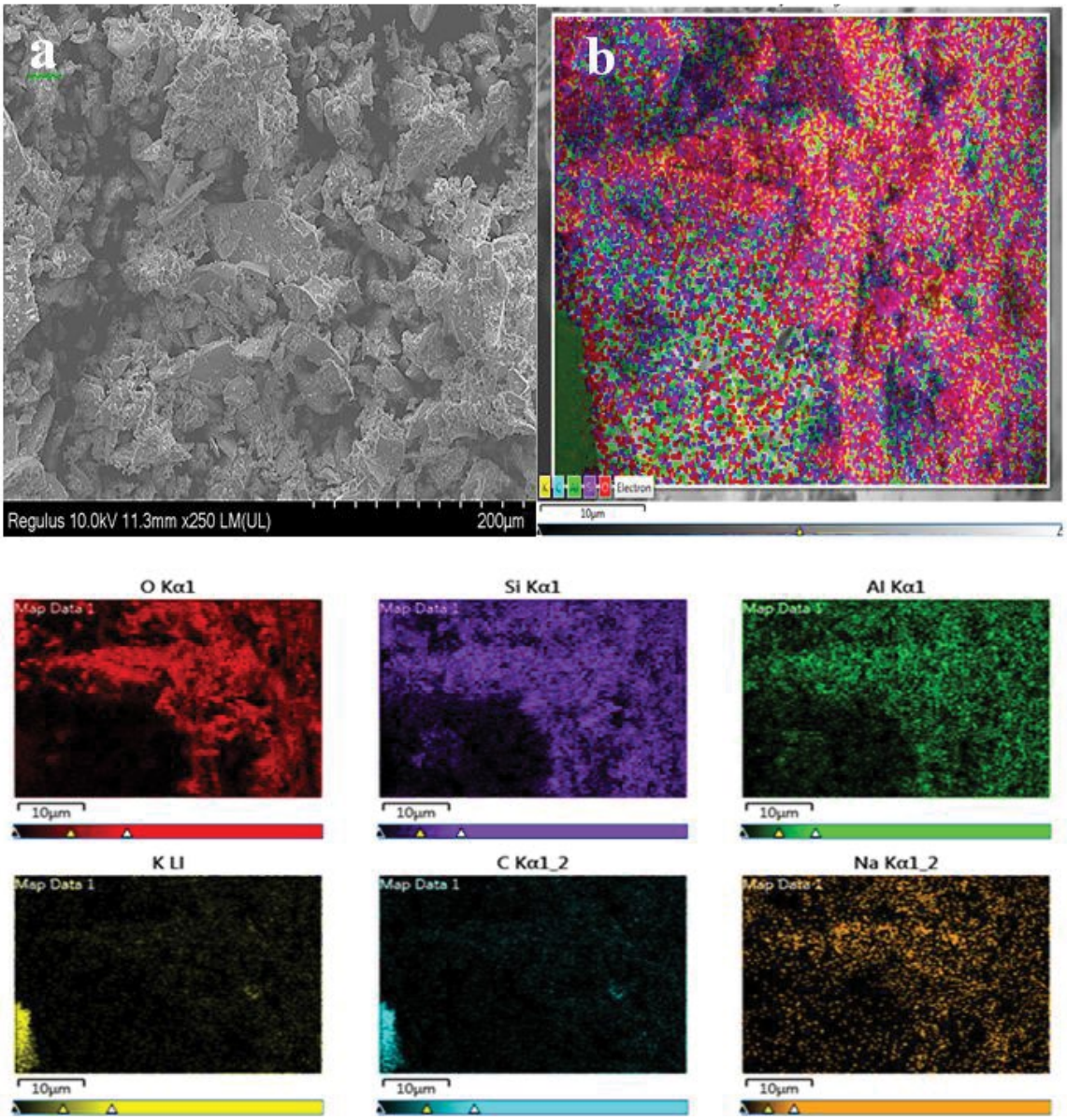

Fig. 5. (a) SEM images and (b) elemental mapping of waste perlite.

of pH on the methylene blue adsorption. Experiments were repeated at an initial concentration of 250 mg/L, as the pH effect could not be observed at 100 mg/L concentration. The change of the adsorbed dyestuff amount with the pH value is given in Fig. 6.

The adsorption of methylene blue on waste perlite increased with the increasing solution pH at the initial concentration of 250 mg/L. This effect can be explained by the cationic dyestuff species' electrostatic interaction with the adsorption sites that are negatively charged. Electrostatic attraction force increases with increasing negative surface charge of the adsorbent. Alkan et al. [18] and Doğan et al. [53] showed that the perlite surface does not have a zero load point but exhibits negative zeta potential in the studied pH range of 3–11. The increase in dyestuff solution's pH increases the adsorption of dyestuff cations on the perlite surface which becomes more negatively charged with the increasing pH [2,22,23]. As seen in Fig. 6, the effect of pH could not be seen for 0.5 g waste perlite amount and 100 mg/L concentration. At this concentration, dye removal increased from 98.33% to 99.08% with the increase in pH from 2.55 to 10.29. In the experiments conducted with 0.5 g waste perlite and 250 mg/L methylene blue concentration, the removal increased from 30.85% to 43.21% with the increase of pH from 2.36 to 11.01. Although the removal increases slightly with the increase in the solution pH, no significant change was observed. Therefore, other experiments were carried out with 100 mg/L initial concentration at the original pH (6.80) of the solution. Similar effects have been shown for the adsorption of methylene blue on perlite [22,23].

3.3. Effect of the adsorbent dosage

The amount of the adsorbent is an important parameter for the adsorption process and enables the capacity of an adsorbent to be determined for a given initial concentration [24]. In order to examine the effect of the adsorbent dosage, 0.1, 0.3, 0.5, 0.7 and 1.0 g waste perlite was added, respectively, to each of the flasks containing the dyestuff solutions with 100 mg/L initial concentration in 50 mL volume, and then the flasks were shaken in a water bath at 25°C for 24 h. The results found are given in Fig. 7.

As shown in Fig. 7, when the amount of adsorbent increases from 0.1 to 1 g, the dyestuff removal increased from 40% to 99%. This is due to the fact that the number of active sites and the surface area increase with the increasing amount of adsorbent. In this way, it is easier for dyestuff molecules to migrate towards the surface and into the interior parts. It was observed that the adsorbent dose did not affect the adsorption efficiency for the adsorbent amounts higher than 0.5 g. Even if the amount of adsorbent was increased above this amount, some of the active sites remained empty since the initial concentration is kept constant; so the % removal did not change [14]. Actually, a very high removal percentage of 99% was reached in the case of using 0.5 g waste perlite, as the adsorbent, as can obviously be seen in Fig. 7. Thus, 0.5 g/50 mL of adsorbent was determined as the optimum amount of the adsorbent. Similar effects have also been reported in the related literature [2,9,12,15,21,24,54].

3.4. Effect of contact time and adsorption kinetics

In order to examine the effect of contact time, 0.5 g of waste perlite was added to each of the methylene blue solutions with a volume of 50 mL and initial concentration of 100 mg/L, and then the flasks containing the solutions were kept in a shaking water bath at 25°C for various times (0.5–24 h).

The cationic structure of methylene blue is effective in the adsorption onto the perlite surface. It can be assumed that the mechanism at work in removing dyestuff from solution involves four steps. The first is the migration of the dyestuff from the solution mass to the adsorbent's outer surface. The second is the diffusion from the boundary layer to the surface of the adsorbent, the third is the adsorption of dyestuff molecules in an active area on the perlite surface, and the fourth is the intraparticle diffusion of the dyestuff into the perlite inner pores. As can be seen in Fig. 8, it was found that the adsorption was fast in the first period of the contact time and then became slow and stagnant with the increase in contact time. This result is due to the Van der Waals forces and electrostatic attraction between the dyestuff molecule and the

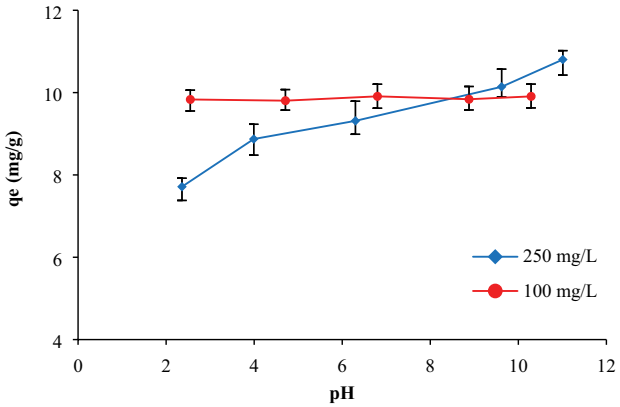

Fig. 6. Effect of solution pH on methylene blue adsorption (T = 25°C, adsorbent dose = 0.5 g, t = 24 h).

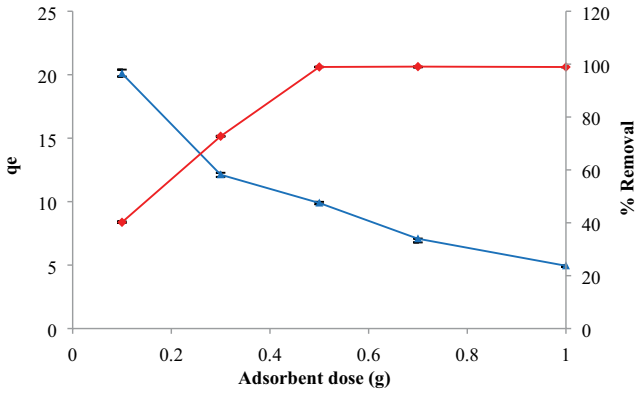

Fig. 7. Effect of the adsorbent dose on methylene blue adsorption (C_0 = 100 mg/L, T = 25°C, t = 24 h, pH = 6.80).

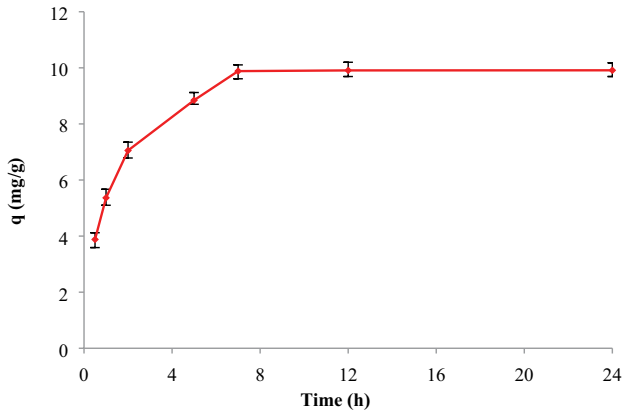

Fig. 8. Effect of contact time on methylene blue removal by waste perlite (C_0 = 100 mg/L, T = 25°C, adsorbent dose = 0.5 g, pH = 6.80).

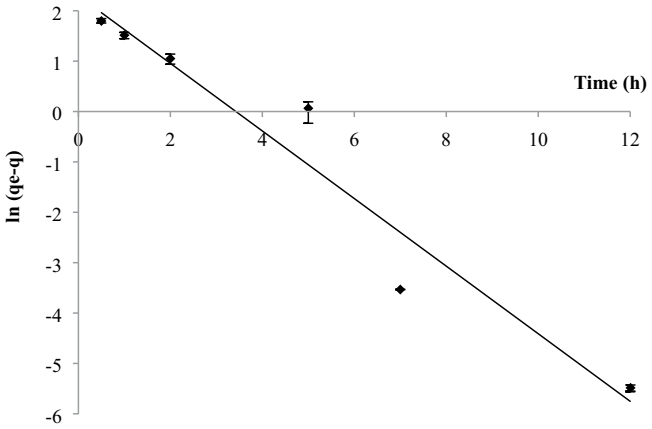

Fig. 9. Adsorption kinetics for pseudo-first-order Lagergren equation (C_0 = 100 mg/L, T = 25°C, adsorbent dose = 0.5 g, pH = 6.80).

adsorbent. The rapid diffusion of the dyestuff molecules on the outer surface was followed by rapid pore diffusion into the intra-particle matrix where the achieved adsorption reached equilibrium rapidly [55]. In the experiments carried out for 24 h, it was observed that the adsorption reached equilibrium in 7 h. After 7 h, there was no significant change in q and % removal, and maximum values of q = 9.91 mg/g and 99.12% removal were reached. Generally, the early times of adsorption are faster when the adsorption involves a surface reaction. Subsequently, a slower adsorption rate occurs as the active adsorption sites decrease [56].

The kinetic data obtained for adsorption were analyzed according to the pseudo-first-order and pseudo-second-order kinetic equations proposed by Lagergren to determine the adsorption rate constant and order. The results are given in Figs. 9, 10 and Table 3.

The adsorbate molecules are most likely transported from the bulk part of the solution to the solid phase via an intraparticle diffusion process; this is often a speed-limiting step. Therefore, the probability of intraparticle diffusion investigated by the intraparticle diffusion model and its results are given in Fig. 11 and Table 3.

The pseudo-first-order Lagergren rate constant is k_1 = 0.671 h^{-1}, pseudo-second-order rate constant is k_2 = 0.139 g/mg/h. By looking at the correlation coefficients, we can say that the adsorption process is more suitable for the pseudo-second-order rate equation. Also, the q_e values found experimentally are more suitable with the q_e values calculated from the pseudo-second-order kinetic model. When the intraparticle diffusion model was examined, it seen that the three phases were formed in the intraparticle diffusion plot, it is indicating that the sorption process proceeds with surface bonding and intraparticle diffusion. In the last step of the plot, diffusion started to slow down due to the decreasing concentration of remaining substance in the solution. The slope of the q_t vs. $t^{1/2}$ plot is defined by the intraparticle diffusion parameter k_i. When the diffusion coefficients were examined, it was seen that the coefficient of the last step has the smallest value with 0.0015 mg/g $min^{1/2}$. This result indicates that the last step was the control step of the adsorption. It can be say that the intraparticle diffusion is one step of the adsorption process, but not the only speed controlling step. These results show that the pseudo-second-order adsorption mechanism is dominant, and chemical adsorption is the rate-limiting step in the methylene blue adsorption process. These results also confirm that the adsorption of methylene blue on the adsorbent is a multi-step process involving adsorption at the outer surface and intraparticle diffusion. Similar results were found for methylene blue adsorption with various adsorbents [4,14,15,21,55].

3.5. Effect of temperature and initial concentration

The effect of initial dyestuff concentration on adsorption was investigated with the effect of temperature. The dyestuff solutions prepared in the concentration range of 10–100 mg/L were adsorbed to the 0.1 g perlite waste at different temperatures. The temperature has two main effects on the adsorption process. It is known that, with the increasing temperature, the diffusion rate of the dyestuff molecules along with the outer boundary layer increase. The dye molecules diffuse more easily in the adsorbent's inner pores with increasing temperature due to the decrease in the solution's viscosity. Also, the equilibrium capacity of the adsorbent increases with increasing temperature [55]. In this study, the amount of adsorbed dyestuff increased with increasing initial concentration. As the concentration of dyestuff in the solution increased, it became easier for the dye molecules to fill the empty centres on the adsorbent surface [2]. Fig. 12 shows the equilibrium isotherms for the adsorption of methylene blue onto waste perlite at different temperatures. The isotherm rise with a greater slope at low C_e and q_e values in the early stages. This indicates that the initial time of adsorption, there are many accessible active sites [36]. The reason for the formation of a flat plateau at higher C_e values is the formation of a monolayer coating on the waste perlite. The adsorption capacity of waste perlite increased with temperature. This result indicates that the adsorption process is endothermic when the

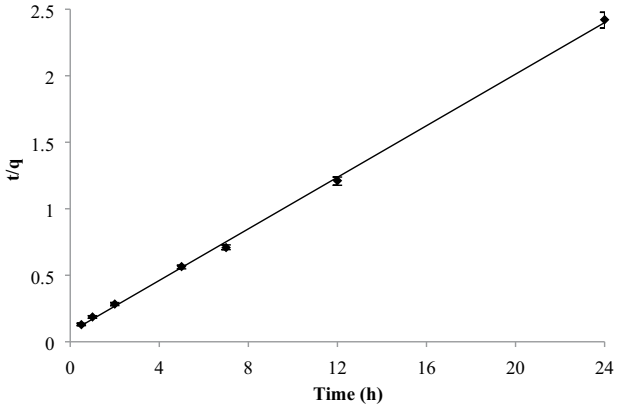

Fig. 10. Adsorption kinetics according to pseudo-second-order rate equation (C_0 = 100 mg/L, T = 25°C, adsorbent dose = 0.5 g, pH = 6.80).

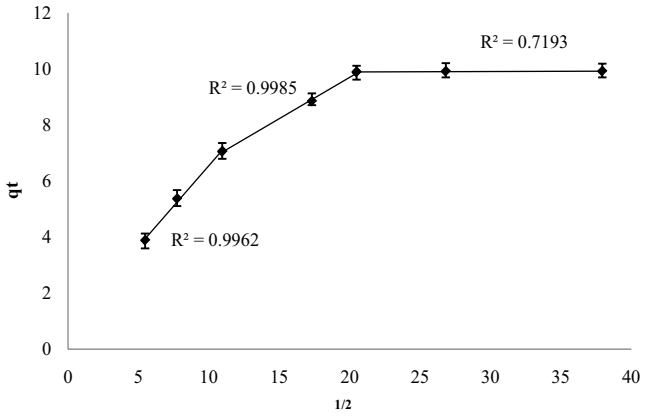

Fig. 11. Intraparticle diffusion model (C_0 = 100 mg/L, T = 25°C, adsorbent dose = 0.5 g, pH = 6.80).

temperature rises from 25°C to 45°C. This effect may be due to the fact that the mobility of dyestuff ions increases with temperature and swelling occurs in the perlite's inner structure. By this way, it becomes easier for methylene blue to penetrate into the perlite's inner parts [22,57]. In addition, with the increase in temperature, the molecules have enough energy to interact with the active sites on the surface [36,58]. The removal percentage was higher at lower dye concentration at all temperatures. It was observed that at higher initial concentrations, the adsorption yields decreased. This low efficiency may be due to the formation of a single layer on the perlite surface which becomes saturated with dye molecules [9,21]. When the initial dyestuff concentration rised from 10 to 100 mg/L, the % removal of dyestuff decreased from 90% to 25%, from 93% to 25% and from 91% to 24% at 25°C, 35°C and 45°C, respectively.

Adsorption isotherms are used to determine the adsorption mechanism and maximum adsorption capacity. The Langmuir and Freundlich isotherms were drawn for the temperatures of 25°C, 35°C and 45°C, and the isotherm constants were calculated for each temperature. The Langmuir and Freundlich isotherms, plotted for the adsorption of

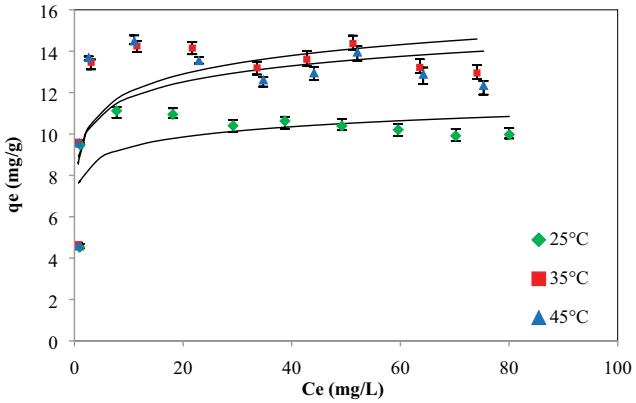

Fig. 12. Effect of initial concentration and temperature on adsorption (adsorbent dose = 0.1 g, t = 24 h, pH = 6.80).

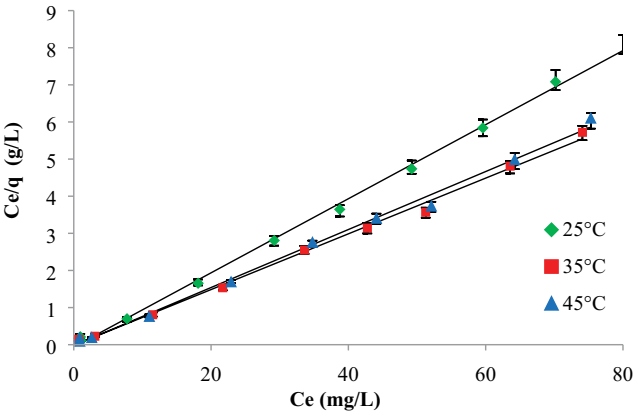

Fig. 13. Langmuir adsorption isotherms at different temperatures.

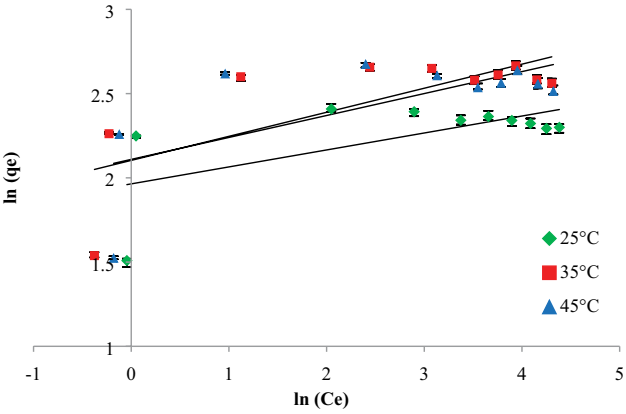

Fig. 14. Freundlich adsorption isotherms at different temperatures.

methylene blue at different temperatures, are shown in Figs 13 and 14, respectively.

The constants of the Langmuir and Freundlich equations are given in Table 4. When R^2 values were compared,

Table 4
Langmuir and Freundlich constants for different temperature

Temperature (°C)	Langmuir				Freundlich		
	Q_0 (mg/g)	b (L/mg)	R^2	R_L	K_f	$1/n$	R^2
25	11.96	0.447	0.972	0.058	7.19	0.121	0.452
35	14.26	1.350	0.966	0.020	8.02	0.157	0.564
45	12.80	3.502	0.995	0.008	8.24	0.130	0.439

Table 5
Comparison of dye adsorption studies with perlite and different clays

Adsorbent	Dye	q_m (mg/g)	Reference
Raw perlite	Congo red	31.84	[44]
Raw perlite	Methylene blue	8.78	[23]
Raw perlite	Commercial synt. dye (magenta)	15.15	[59]
Raw perlite	Methylene blue	0.455	[60]
Raw perlite	Basic blue 41	7.97	[61]
Expanded perlite	Rhodamine B	0.49	[48]
Expanded perlite	Methylene blue	1.18	[62]
Expanded perlite	Malachite green	9.91	[2]
Expanded perlite	Methylene blue	0.365	[60]
Expanded perlite	Basic blue 41	9.08	[61]
Unexpanded perlite	Methylene blue	155	[22]
Montmorillonite	Methylene blue	289.12	[63]
Kaolinite	Methylene blue	52.76	[64]
Sepiolite	Methylene blue	79.37	[65]
Zeolite	Methylene blue	55.33	[66]
This study	Methylene blue	9.91	

Table 6
Thermodynamic parameters for the adsorption of methylene blue onto waste perlite

			ΔG (kJ/mol K)		
R^2	ΔH (kJ/mol)	ΔS (kJ/mol K)	298 K	308 K	318 K
0.9994	32.975	0.1181	–2.218	–3.399	–4.580

it was seen that the Langmuir equation fits the experimental data better. The Langmuir isotherm's good compatibility may indicate that single-layer adsorption occurs at homogeneously distributed active points on the perlite surface [2,20].

The R_L value explains whether the isotherm is unfavourable ($R_L > 1$), favourable ($R_L < 1$), linear ($R_L = 1$) or irreversible ($R_L = 0$) for the adsorbent. If the average of the R_L values for each of the different initial concentrations used is between 0 and 1, it indicates that adsorption is favorable. The calculated R_L values were found favourable as $0 < R_L < 1$ at all temperatures and all initial concentrations (Table 4). Therefore, perlite can be considered as a suitable adsorbent material for methylene blue adsorption. Similar results were found in some previous studies with methylene blue [5,54]. And in Table 5 a comparative study of some dyestuff adsorption studies with perlite and other clays is summarized.

As seen in the table, the maximum adsorption capacity of the adsorbent is highly dependent on the properties of the perlite, operating conditions and the structure of the dyestuff. Perlite has the ability to remove the methylene blue from an aqueous solution.

3.6. Adsorption thermodynamics

As shown in Table 6, the positive values of $\Delta H°$ indicate that the adsorption of methylene blue on perlite waste is an endothermic process. The positive $\Delta S°$ value indicates that the attraction of methylene blue towards perlite is good, thanks to the structural changes in methylene blue and perlite. Irregularity increases during chemical adsorption at the

liquid–solid interface, and the positive $\Delta S°$ value is an indicator of this. The $\Delta G°$ value decreases with increasing temperature. This indicates that the driving force is greater at high temperatures, and this effect causes the adsorption capacity to increase with increasing temperature. Similar results were found in some previous studies on methylene blue adsorption onto different adsorbents and perlite [11,15,67–70].

4. Conclusion

In this study, the removal of dyestuff in wastewater using waste perlite by adsorption method was investigated. Waste perlite supplied from a factory producing expanded perlite was used as an adsorbent in adsorption. Methylene blue, a cationic (basic) dye, is used as the dyestuff. The effects of pH, adsorbent dose, contact time, initial concentration and temperature, which are factors affecting adsorption, were investigated. According to the results, since no significant difference was observed in the amount of dye removal with the change of solution pH, the solution's original pH = 6.80 was applied in all experiments. In the experiments where the effect of the adsorbent dose was examined, it was determined that the most suitable amount of adsorbent was 0.5 g per 50 mL dye solution at 100 mg/L concentration. It was observed that the system stabilized in 7 h when the adsorption experiments were carried out for 24 h. The kinetic and thermodynamic constants were determined for the adsorption of the dyestuff onto the perlite waste. The kinetic data show that the adsorption of methylene blue onto waste perlite takes place in more than one step. The step that limits the adsorption rate fits the pseudo-second-order kinetic model. The thermodynamic data show that this process is endothermic and spontaneous. The Langmuir and Freundlich adsorption isotherm models and regression analysis showed that the most suitable isotherm was the Langmuir model. It was also showed that single layer adsorption occurred in homogeneously distributed active sites on the perlite surface. In this study, it is focused on the evaluation of a waste material as a new adsorbent. It was thought that the unexpanded perlite remaining after the expansion process could be used as an adsorbent in dye adsorption. As a result of the study, it can be said that the waste perlite used is a suitable adsorbent for the removal of methylene blue, a cationic dyestuff, from wastewater. Regeneration and reuse is an important advantage for an adsorbent to be economical. For this reason, it is recommended to perform a desorption/regeneration study after adsorption.

References

[1] T. Robinson, G. McMullan, R. Marchant, P. Nigam, Remediation of dyes in textile effluent: a critical review on current treatment technologies with a proposed alternative, Bioresour. Technol., 77 (2001) 247–255.

[2] U. Selengil, T.E. Bektaş, Investigation of the usability of perlite waste for dyestuff removal from aqueous solution, Sakarya Univ. J. Sci., 24 (2020) 224–230.

[3] Y. Wu, L. Zhang, C. Gao, J. Ma, X. Ma, R. Han, Adsorption of copper ions and methylene blue in a single and binary system on wheat straw, J. Chem. Eng. Data, 54 (2009) 3229–3234.

[4] T. Liu, Y. Li, Q. Du, J. Sun, Y. Jiao, G. Yang, Z. Wang, Y. Xia, W. Zhang, K. Wang, Adsorption of methylene blue from aqueous solution by graphene, Colloids Surf., B, 90 (2012) 197–203.

[5] B. Hameed, A.M. Din, A. Ahmad, Adsorption of methylene blue onto bamboo-based activated carbon: kinetics and equilibrium studies, J. Hazard. Mater., 141 (2007) 819–825.

[6] V. Vadivelan, K.V. Kumar, Equilibrium, kinetics, mechanism, and process design for the sorption of methylene blue onto rice husk, J. Colloid Interface Sci., 286 (2005) 90–100.

[7] L.A. da Silva, S.M.S. Borges, P.N. Paulino, M.A. Fraga, S.T. de Oliva, S.G. Marchetti, M. do Carmo Rangel, Methylene blue oxidation over iron oxide supported on activated carbon derived from peanut hulls, Catal. Today, 289 (2017) 237–248.

[8] A. Jain, V. Gupta, A. Bhatnagar, Utilization of industrial waste products as adsorbents for the removal of dyes, J. Hazard. Mater., 101 (2003) 31–42.

[9] M.M. Karim, A.K. Das, S.H. Lee, Treatment of colored effluent of the textile industry in Bangladesh using zinc chloride treated indigenous activated carbons, Anal. Chim. Acta, 576 (2006) 37–42.

[10] Y. Önal, C. Akmil-Başar, D. Eren, Ç. Sarıcı-Özdemir, T. Depci, Adsorption kinetics of malachite green onto activated carbon prepared from Tunçbilek lignite, J. Hazard. Mater., 128 (2006) 150–157.

[11] S. Tahir, N. Rauf, Removal of a cationic dye from aqueous solutions by adsorption onto bentonite clay, Chemosphere, 63 (2006) 1842–1848.

[12] A. Özer, G. Dursun, Removal of methylene blue from aqueous solution by dehydrated wheat bran carbon, J. Hazard. Mater., 146 (2007) 262–269.

[13] B. Kayranli, Adsorption of textile dyes onto iron based waterworks sludge from aqueous solution; isotherm, kinetic and thermodynamic study, Chem. Eng. J., 173 (2011) 782–791.

[14] P.M.K. Reddy, P. Verma, C. Subrahmanyam, Bio-waste derived adsorbent material for methylene blue adsorption, J. Taiwan Inst. Chem. Eng., 58 (2016) 500–508.

[15] Z. Li, G. Wang, K. Zhai, C. He, Q. Li, P. Guo, Methylene blue adsorption from aqueous solution by loofah sponge-based porous carbons, Colloids Surf., A, 538 (2018) 28–35.

[16] B. Acemioğlu, Adsorption of Congo red from aqueous solution onto calcium-rich fly ash, J. Colloid Interface Sci., 274 (2004) 371–379.

[17] E.A. Abdelrahman, Synthesis of zeolite nanostructures from waste aluminum cans for efficient removal of malachite green dye from aqueous media, J. Mol. Liq., 253 (2018) 72–82.

[18] M. Alkan, Ö. Demirbaş, M. Doğan, Adsorption kinetics and thermodynamics of an anionic dye onto sepiolite, Microporous Mesoporous Mater., 101 (2007) 388–396.

[19] F. Largo, R. Haounati, S. Akhouairi, H. Ouachtak, R. El Haouti, A. El Guerdaoui, N. Hafid, D.M.F. Santos, F. Akbal, A. Kuleyin, A. Jada, A.A. Addi, Adsorptive removal of both cationic and anionic dyes by using sepiolite clay mineral as adsorbent: experimental and molecular dynamic simulation studies, J. Mol. Liq., 318 (2020) 114247, doi: 10.1016/j.molliq.2020.114247.

[20] E. González Pradas, M. Villafranca Sánchez, F. Cantón Cruz, M. Socías Viciana, M. Fernández Pérez, Adsorption of cadmium and zinc from aqueous solution on natural and activated bentonite, J. Chem. Technol. Biotechnol., 59 (1994) 289–295.

[21] S. Yorgun, N. Karakehya, D. Yıldız, Adsorption of methylene blue onto activated carbon obtained from $ZnCl_2$, Desal. Water Treat., 58 (2017) 274–284.

[22] M. Doğan, M. Alkan, Y. Onganer, Adsorption of methylene blue from aqueous solution onto perlite, Water Air Soil Pollut., 120 (2000) 229–248.

[23] M. Doğan, M. Alkan, A. Türkyilmaz, Y. Özdemir, Kinetics and mechanism of removal of methylene blue by adsorption onto perlite, J. Hazard. Mater., 109 (2004) 141–148.

[24] A. Sarı, M. Tuzen, D. Cıtak, M. Soylak, Adsorption characteristics of Cu(II) and Pb(II) onto expanded perlite from aqueous solution, J. Hazard. Mater., 148 (2007) 387–394.

[25] Z. Talip, M. Eral, Ü. Hiçsönmez, Adsorption of thorium from aqueous solutions by perlite, J. Environ. Radioact., 100 (2009) 139–143.

[26] M. Rafatullah, O. Sulaiman, R. Hashim, A. Ahmad, Adsorption of methylene blue on low-cost adsorbents: a review, J. Hazard. Mater., 177 (2010) 70–80.

[27] S. Saja, A. Bouazizi, B. Achiou, M. Ouammou, A. Albizane, J. Bennazha, S.A. Younssi, Elaboration and characterization of low-cost ceramic membrane made from natural Moroccan perlite for treatment of industrial wastewater, J. Environ. Chem. Eng., 6 (2018) 451–458.
[28] H. Xu, W. Jia, S. Ren, J. Wang, Novel and recyclable demulsifier of expanded perlite grafted by magnetic nanoparticles for oil separation from emulsified oil wastewaters, Chem. Eng. J., 337 (2018) 10–18.
[29] H. Joolaei, M. Vossoughi, A.R.M. Abadi, A. Heravi, Removal of humic acid from aqueous solution using photocatalytic reaction on perlite granules covered by nano TiO_2 particles, J. Mol. Liq., 242 (2017) 357–363.
[30] H. Rizk, I. Ahmed, S. Metwally, Selective sorption and separation of molybdenum ion from some fission products by impregnated perlite, Chem. Eng. Process. Process Intensif., 124 (2018) 131–136.
[31] G. Jia, Z. Li, P. Liu, Q. Jing, Preparation and characterization of aerogel/expanded perlite composite as building thermal insulation material, J. Non-Cryst. Solids, 482 (2018) 192–202.
[32] A.S. Gandage, V.R.V. Rao, M.V.N. Sivakumar, A. Vasan, M. Venu, A.B. Yaswanth, Effect of perlite on thermal conductivity of self compacting concrete, Procedia – Soc. Behav. Sci., 104 (2013) 188–197.
[33] Y. Kar, Catalytic pyrolysis of car tire waste using expanded perlite, Waste Manage., 31 (2011) 1772–1782.
[34] A. Hamza, I. Kocserha, The effect of expanded perlite on fired clay bricks, J. Phys. Conf. Ser., 1527 (2020) 012032.
[35] A. Georgiev, A. Yoleva, S. Djambazov, D. Dimitrov, V. Ivanova, Effect of expanded vermiculite and expanded perlite as pore forming additives on the physical properties and thermal conductivity of porous clay bricks, J. Chem. Technol. Metall., 53 (2018) 275–280.
[36] H. Demiral, İ. Demiral, F. Tümsek, B. Karabacakoğlu, Adsorption of chromium(VI) from aqueous solution by activated carbon derived from olive bagasse and applicability of different adsorption models, Chem. Eng. J., 144 (2008) 188–196.
[37] A. Sharma, K.G. Bhattacharyya, Adsorption of chromium(VI) on *Azadirachta indica* (Neem) leaf powder, Adsorption, 10 (2005) 327–338.
[38] S. Shakoor, A. Nasar, Removal of methylene blue dye from artificially contaminated water using citrus limetta peel waste as a very low cost adsorbent, J. Taiwan Inst. Chem. Eng., 66 (2016) 154–163.
[39] H. Yuh-Shan, Citation review of Lagergren kinetic rate equation on adsorption reactions, Scientometrics, 59 (2004) 171–177.
[40] D. Kavitha, C. Namasivayam, Experimental and kinetic studies on methylene blue adsorption by coir pith carbon, Bioresour. Technol., 98 (2007) 14–21.
[41] F. Chen, M. Zhang, L. Ma, J. Ren, P. Ma, B. Li, N. Wu, Z. Song, L. Huang, Nitrogen and sulfur codoped micro-mesoporous carbon sheets derived from natural biomass for synergistic removal of chromium(VI): adsorption behavior and computing mechanism, Sci. Total Environ., 730 (2020) 138930, doi: 10.1016/j.scitotenv.2020.138930.
[42] S. Kabra, S. Katara, A. Rani, Characterization and study of Turkish perlite, Int. J. Innov. Res. Sci. Eng. Technol., 2 (2013) 4319–4326.
[43] A.A. Reka, B. Pavlovski, K. Lisichkov, A. Jashari, B. Boev, I. Boev, M. Lazarova, V. Eskizeybek, A. Oral, P. Makreski, Chemical, mineralogical and structural features of native and expanded perlite from Macedonia, Geologia Croatica, 72 (2019) 215–221.
[44] G. Vijayakumar, M. Dharmendirakumar, S. Renganathan, S. Sivanesan, G. Baskar, K.P. Elango, Removal of Congo red from aqueous solutions by perlite, Clean–Soil, Air, Water, 37 (2009) 355–364.
[45] S.K. Malpani, D. Goyal, S. Katara, A. Rani, Turkish perlite supported nickel oxide as the heterogeneous acid catalyst for a series of Claisen? Schmidt condensation reactions, Turk. J. Chem., 45 (2021) 1097–1114.
[46] D. Goyal, R. Hada, S. Katara, A. Bhatia, S.K. Malpani, Development of green, effective, and cost-efficient perlite supported solid base catalyst and application in condensation reactions, Mater. Today:. Proc., 49 (2022) 3717–3725.
[47] A. Aziz, A. Benzaouak, A. Bellil, T. Alomayri, I.-E.E.N. el Hassani, M. Achab, H. El Azhari, Y. Et-Tayea, F.U.A. Shaikh, Effect of acidic volcanic perlite rock on physio-mechanical properties and microstructure of natural pozzolan based geopolymers, Case Stud. Constr. Mater., 15 (2021) e00712.
[48] B. Damiyine, A. Guenbour, R. Boussen, Adsorption of rhodamine B dye onto expanded perlite from aqueous solution: kinetics, equilibrium and thermodynamics, J. Mater. Environ. Sci., 8 (2017) 345–355.
[49] A.G. Celik, A.M. Kilic, G.O. Cakal, Expanded perlite aggregate characterization for use as a lightweight construction raw material, Physicochem. Probl. Miner. Process., 49 (2013) 689–700.
[50] M. Gürsoy, M. Karaman, Hydrophobic coating of expanded perlite particles by plasma polymerization, Chem. Eng. J., 284 (2016) 343–350.
[51] E. Rostami, R. Norouzbeigi, A. Rahbar-Kelishami, A comparative study of malachite green removal from an aqueous solution using raw and chemically modified expanded perlite, J. Part Sci. Technol., 3 (2017) 79–87.
[52] M. Roulia, K. Chassapis, J. Kapoutsis, E. Kamitsos, T. Savvidis, Influence of thermal treatment on the water release and the glassy structure of perlite, J. Mater. Sci., 41 (2006) 5870–5881.
[53] M. Doğan, M. Alkan, Ü. Çakir, Electrokinetic properties of perlite, J. Colloid Interface Sci., 192 (1997) 114–118.
[54] D. Ghosh, K.G. Bhattacharyya, Adsorption of methylene blue on kaolinite, Appl. Clay Sci., 20 (2002) 295–300.
[55] M. Doğan, H. Abak, M. Alkan, Adsorption of methylene blue onto hazelnut shell: kinetics, mechanism and activation parameters, J. Hazard. Mater., 164 (2009) 172–181.
[56] C.-H. Weng, Y.-F. Pan, Adsorption characteristics of methylene blue from aqueous solution by sludge ash, Colloids Surf., A, 274 (2006) 154–162.
[57] H. Asfour, O. Fadali, M. Nassar, M. El-Geundi, Equilibrium studies on adsorption of basic dyes on hardwood, J. Chem. Technol. Biotechnol., 35 (1985) 21–27.
[58] E. Malkoc, Y. Nuhoglu, Potential of tea factory waste for chromium(VI) removal from aqueous solutions: thermodynamic and kinetic studies, Sep. Purif. Technol., 54 (2007) 291–298.
[59] S. Sawasdee, Adsorption of dyestuff in household-scale onto Lopburi pumiceous perlite, 35–47.
[60] S.M. Turp, N. Ekinci, Methylene blue dye adsorption isotherms and kinetics via porous materials natural and expanded perlite, Fresenius Environ. Bull., 30 (2021) 13058–13071.
[61] M. Roulia, A.A. Vassiliadis, Sorption characterization of a cationic dye retained by clays and perlite, Microporous Mesoporous Mater., 116 (2008) 732–740.
[62] X. Zhao, Y. Li, X. Li, H. Luo, H. Zhang, Removal of Methylene Blue From Aqueous Solution Using Expanded Perlite, Proceedings of the 2017 5th International Conference on Mechatronics, Materials, Chemistry and Computer Engineering (ICMMCCE 2017), Atlantis Press, 2017, pp. 434–441.
[63] C. Almeida, N. Debacher, A. Downs, L. Cottet, C. Mello, Removal of methylene blue from colored effluents by adsorption on montmorillonite clay, J. Colloid Interface Sci., 332 (2009) 46–53.
[64] L. Mouni, L. Belkhiri, J.-C. Bollinger, A. Bouzaza, A. Assadi, A. Tirri, F. Dahmoune, K. Madani, H. Remini, Removal of Methylene blue from aqueous solutions by adsorption on kaolin: kinetic and equilibrium studies, Appl. Clay Sci., 153 (2018) 38–45.
[65] İ. Küncek, S. Şener, Adsorption of methylene blue onto sonicated sepiolite from aqueous solutions, Ultrason. Sonochem., 17 (2010) 250–257.
[66] S. Wang, H. Li, L. Xu, Application of zeolite MCM-22 for basic dye removal from wastewater, J. Colloid Interface Sci., 295 (2006) 71–78.
[67] S. Hong, C. Wen, J. He, F. Gan, Y.-S. Ho, Adsorption thermodynamics of methylene blue onto bentonite, J. Hazard. Mater., 167 (2009) 630–633.

[68] J. Pang, F. Fu, Z. Ding, J. Lu, N. Li, B. Tang, Adsorption behaviors of methylene blue from aqueous solution on mesoporous birnessite, J. Taiwan Inst. Chem. Eng., 77 (2017) 168–176.
[69] H. Zhang, Y. Tang, X. Liu, Z. Ke, X. Su, D. Cai, X. Wang, Y. Liu, Q. Huang, Z. Yu, Improved adsorptive capacity of pine wood decayed by fungi *Poria cocos* for removal of malachite green from aqueous solutions, Desalination, 274 (2011) 97–104.
[70] P. Demirçivi, G.N. Saygılı, Comparative study of modified expanded perlite with hexadecyltrimethylammonium-bromide and gallic acid for boron adsorption, J. Mol. Liq., 254 (2018) 383–390.